Nanobody-based CAR T cells that target the tumor microenvironment inhibit the growth of solid tumors in immunocompetent mice

Yushu Joy Xie[a,b], Michael Dougan[c], Noor Jailkhani[d], Jessica Ingram[e,1], Tao Fang[a], Laura Kummer[a], Noor Momin[b,d], Novalia Pishesha[a,b], Steffen Rickelt[d], Richard O. Hynes[d,f,g], and Hidde Ploegh[a,2]

[a]Program in Cellular and Molecular Medicine, Boston Children's Hospital, Boston, MA 02115; [b]Department of Biological Engineering, Massachusetts Institute of Technology, Cambridge, MA 02138; [c]Division of Gastroenterology, Massachusetts General Hospital, Boston, MA 02114; [d]Koch Institute for Integrative Cancer Research, Massachusetts Institute of Technology, Cambridge, MA 02138; [e]Department of Cancer Immunology and Virology, Dana-Farber Cancer Institute, Boston, MA 02215; [f]Department of Biology, Massachusetts Institute of Technology, Cambridge, MA 02138; and [g]Howard Hughes Medical Institute, Chevy Chase, MD 20815

Chimeric antigen receptor (CAR) T cell therapy has been successful in clinical trials against hematological cancers, but has experienced challenges in the treatment of solid tumors. One of the main difficulties lies in a paucity of tumor-specific targets that can serve as CAR recognition domains. We therefore focused on developing VHH-based, single-domain antibody (nanobody) CAR T cells that target aspects of the tumor microenvironment conserved across multiple cancer types. Many solid tumors evade immune recognition through expression of checkpoint molecules, such as PD-L1, that down-regulate the immune response. We therefore targeted CAR T cells to the tumor microenvironment via the checkpoint inhibitor PD-L1 and observed a reduction in tumor growth, resulting in improved survival. CAR T cells that target the tumor stroma and vasculature through the EIIIB+ fibronectin splice variant, which is expressed by multiple tumor types and on neovasculature, are likewise effective in delaying tumor growth. VHH-based CAR T cells can thus function as antitumor agents for multiple targets in syngeneic, immunocompetent animal models. Our results demonstrate the flexibility of VHH-based CAR T cells and the potential of CAR T cells to target the tumor microenvironment and treat solid tumors.

chimeric antigen receptor | tumor microenvironment | immunotherapy

Cancers can avoid eradication by evading, and sometimes actively suppressing, the immune system, although they are often initially recognizable by immune cells. The rapidly evolving field of immunotherapy targets cancers by harnessing the power of the immune system. A key player in that approach is the chimeric antigen receptor (CAR) T cell (1–3). CAR T cells are T cells into which a recombinant receptor has been introduced to redirect their specificity toward an antigen of choice. Such receptors comprise an extracellular module that recognizes antigen independent of MHC restriction, in combination with cytoplasmic signaling domains. The antigen recognition module of CAR T cells is usually a single-chain variable fragment (scFv), linked to a costimulatory domain and a cytoplasmic activation domain, such as the CD3ζ or FcRγ intracellular signaling domain (4–6). The scFvs are composed of a heavy-chain variable fragment connected to a light-chain variable fragment by a flexible linker. They are typically reformatted from a full-length Ig, with the linker optimized to preserve heavy- and light-chain variable region pairing. However, scFvs do not always fold efficiently and can be prone to aggregation (7, 8). In contrast, the variable regions of heavy-chain−only antibodies (VHHs or nanobodies) are small, stable, camelid-derived single-domain antibody fragments with affinities comparable to traditional scFvs (9, 10). VHHs are generally less immunogenic than murine scFvs and, owing to their small size, can access epitopes different from those seen by

scFvs (11–13). VHHs could therefore serve as suitable antigen recognition domains in CAR T cells, and several potentially interesting VHHs (14–16) have been tested. Unlike scFvs, VHHs do not require the additional folding and assembly steps that come with V-region pairing. They allow surface display without the requirement for extensive linker optimization or other types of reformatting. The ability to switch out various VHH-based recognition domains yields a highly modular platform, accessible without having to reformat each new conventional antibody into an scFv.

CAR T cell therapies have proven clinically effective exclusively in hematological cancers. CD19-specific CAR T cells have shown success in treating a number of B cell leukemias and lymphomas, as B cell depletion is comparatively well tolerated (17, 18). However, not all tumors have highly specific biomarkers or antigens that are shared by dispensable cell types such as B cells, especially in the case of solid tumors. Antigens such as ErbB2, PSMA, and B7-H3 are considered possible CAR targets

Significance

Despite its success in treating hematological cancers, chimeric antigen receptor (CAR) T cell therapy does not so easily eliminate solid tumors. Solid tumors generally develop in a highly immunosuppressive environment and are difficult to target, mostly due to a lack of tumor-specific antigen expression, but other factors contribute as well. This study develops a strategy to target multiple solid tumor types through markers in their microenvironment. The use of single-domain antibody (VHH)-based chimeric antigen receptor (CAR) T cells that recognize these markers circumvents the need for tumor-specific targets. VHH-based CAR T cells that target the tumor microenvironment through immune checkpoint receptors or through stroma and ECM markers are effective against solid tumors in syngeneic, immunocompetent animal models.

for solid tumors, but expression at low levels elsewhere may compromise such applications (19–21). Indeed, an ErbB2-targeted CAR T cell designed to treat metastatic colon cancer proved lethal in a patient, most likely due to off-tumor targeting of healthy lung epithelial cells (19). Off-tumor effects can include widespread cytokine release, which can lead to organ failure (19–21).

Current CAR T cell therapies target the tumor directly, as in the case of CD19 or mesothelin-specific CAR T cells. However, solid tumors rarely display unique antigenic markers, and exploitation of neoantigens would require their surface expression, as well as the production of immunoglobulins or VHHs that recognize them, to generate appropriately specific CARs. To delay the growth of solid tumors, it may be helpful to compromise their microenvironment. Moreover, the microenvironments of many solid tumors share characteristics, for example, the expression of inhibitory molecules such as PD-L1 (22, 23). Using VHHs as recognition domains, we therefore explored PD-L1−specific CAR T cells to target the tumor microenvironment. PD-L1 is widely expressed on tumor cells, as well as on the infiltrating myeloid cells and lymphocytes. A CAR that recognizes PD-L1 should relieve immune inhibition and at the same time allow CAR T cell activation in the tumor microenvironment. PD-L1−targeted CAR T cells might thus reprogram the tumor microenvironment, dampening immunosuppressive signals and promoting inflammation. To test this concept, we used the fully syngeneic B16 melanoma model, as well as a PD-L1−overexpressing B16 melanoma model and a colon adenocarcinoma cell line, MC38, in immunocompetent mice. Our results show a significant delay in tumor growth and improved survival by treatment with anti−PD-L1 CAR T cells.

The reliance of solid tumors on extracellular matrix (ECM) and on neovasculature for nutrient supply affords yet another possible target for CAR T cells, as tumor ECM and newly formed blood vessels display unique antigens not commonly found in healthy adults (24, 25). As an extension of the concept that targeting PD-L1 in the tumor microenvironment may prove beneficial, we generated CAR T cells using a VHH that recognizes EIIIB, a splice variant of fibronectin strongly expressed in both the tumor ECM and the neovasculature (24, 26). These CAR T cells also reduce the rate of tumor growth in the B16 melanoma model. Attacking the tumor stroma and/or the neovasculature may not only help to establish a local inflammatory response that benefits subsequent immune recognition in a vaccinal manner, but it may also enhance access to the tumor for otherwise impermeant drugs in difficult to treat cancers. Many solid tumors depend on stromal ECM and neovasculature for survival, and, therefore, EIIIB serves as an easily generalizable target that is not limited to a specific tumor type. In this study, we establish VHH-based CAR T cells as a versatile, modular system to target various compartments of the solid tumor microenvironment.

Results

VHH-Based CAR T Cells Expressed with Retention of Antigen Specificity.
The VHH-based CAR T cells generated in this study follow the principal design of scFv-based CAR T cells, where the VHH replaces the scFv as the recognition module. For the construction of these CARs, we used VHHs specific for GFP [referred to as "enhancer" or "Enh" (15)], for PD-L1 (B3 or A12), and for the EIIIB splice variant of fibronectin (NJB2) (14, 27–29). For most experiments, we used 1B7, a VHH that recognizes a *Toxoplasma gondii* kinase, as a negative (nonspecific) control (16). The lentiviral vector backbone is derived from murine stem cell virus and encodes the CAR construct in addition to an internal ribosomal entry site (IRES)-driven green fluorescent protein (GFP) or mCherry cassette to gauge transduction efficiency (Fig. 1A). Before transduction, T cells obtained from spleen were activated with plate-bound anti-mouse CD28 and anti-mouse CD3 (Fig. 1B).
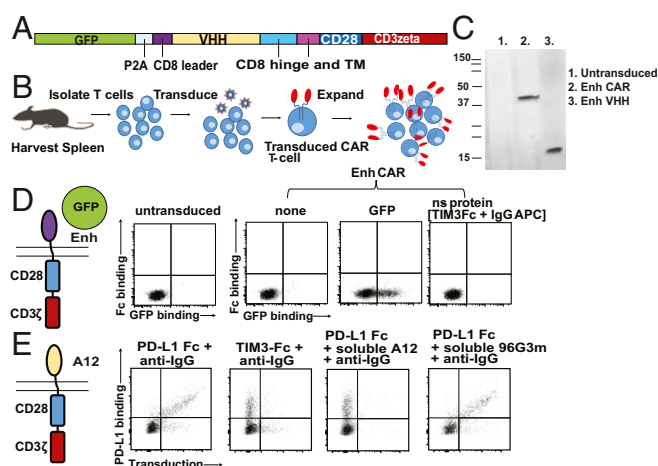

Fig. 1. VHH-based CAR T cells expressed with retention of antigen specificity. (A) Retroviral construct of VHH-based CAR T cells and their introduction into mouse T cells. (B) Production process for generation of CAR T cells. (C) Immunoblot on T cells transduced with Enh CAR construct. Lysates from transduced and untransduced T cells were blotted against using anti-Enh serum generated from immunization of mice with the Enh VHH. Polypeptides corresponding to the Enh CAR and soluble Enh were seen. (D) Schematic of assay to test for Enh CAR display. T cells were transduced with Enh CAR and probed for binding to GFP by flow cytometry. Nonspecific binding was measured by incubation with an irrelevant protein, TIM3−Fc fusion, probed for with an anti-mouse IgG conjugated to APC. (E) T cells were transduced with A12 CAR targeted to PD-L1. Successful display is probed by binding to recombinant PD-L1−Fc fusion and detected by an anti-mouse IgG conjugated to APC.

By gating on those cells that were successfully transduced [GFP or mCherry-positive, typically 40 to 80% transduced (*SI Appendix*, Fig. S1)], we assessed CAR expression and functionality by binding of suitably labeled CAR ligands. Immunoblots with Enh CAR lysate developed with an anti-Enh serum show a polypeptide of ~40 kDa, the expected size of the Enh CAR (Fig. 1C). The Enh CAR, when transduced into T cells, retained the ability to bind GFP, as evident from a FACS-based assay (Fig. 1D). We likewise showed that the anti−PD-L1 CAR, based on the A12 VHH, recognized a recombinant PD-L1−Fc fusion, as detected by fluorescently labeled anti-mouse IgG (Fig. 1E). In all cases, binding of antigen to CAR T cells was blocked by inclusion of a molar excess of the corresponding free VHH as competitor, indicating specificity of ligand binding. We conclude that VHHs are readily displayed as CAR recognition modules with full retention of antigen-binding specificity.

In Vitro Activity of CAR T Cells: Cytokine Production and Cytotoxicity.
Having shown the binding specificity of VHH-based CARs, we next determined the functional properties of VHH-based CAR T cells. Upon incubation of GFP-specific CAR T cells with plate-bound GFP, we observed an increase in IL-2 and IFNγ production in the culture supernatants (Fig. 2 A and B). Even though GFP in solution is a monomer, the plate-bound configuration allows multivalent engagement and ensures activation. Cytotoxicity of the PD-L1−targeted A12 CAR T cells was assessed on B16 melanoma cells, which express PD-L1. The A12 CAR T cells killed the B16 melanoma in a dose-dependent manner (Fig. 2C). IFNγ production from the CAR T cells in response to exposure to the B16 melanoma likewise increased at higher E:T ratios (Fig. 2D). PD-L1 is overexpressed on a number of different tumor types. We showed that the A12 PD-L1−targeted CAR can elicit cytotoxicity against several different cancer cell lines that express PD-L1, including C3.43 (Fig. 2 E and F), an HPV16-transformed cell line, and MC38 (Fig. 2 G and H), a colon
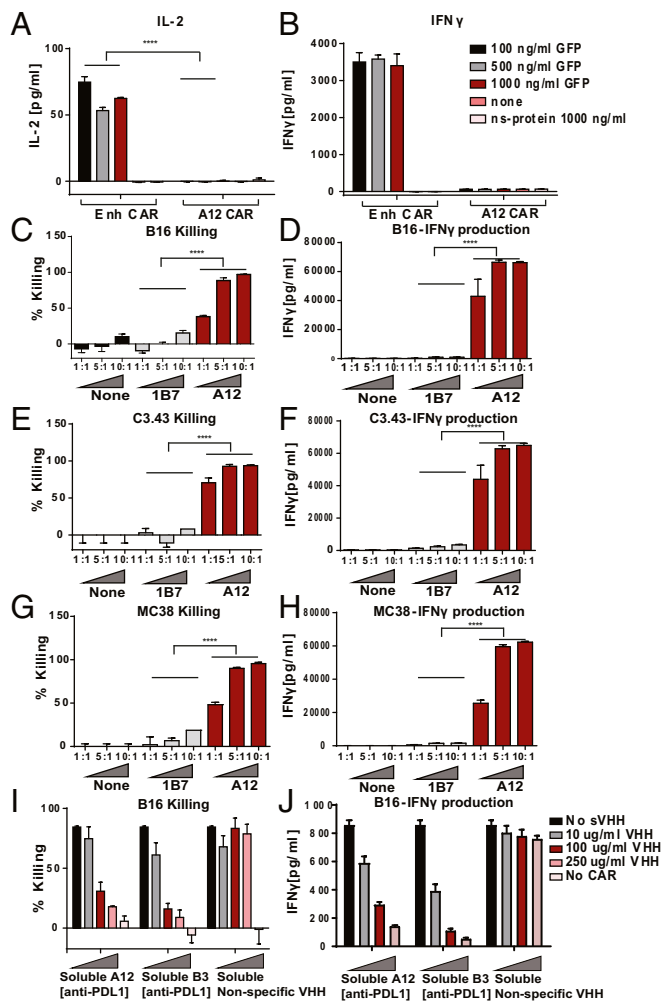
Fig. 2. In vitro activity of CAR T cells: cytokine production and cytotoxicity. T cells were transduced with Enh CAR. (*A*) IL-2 and (*B*) IFNγ levels in the supernatant of CAR T cells cultured for 24 h with GFP or an irrelevant protein (TIM3–Fc). (*C–J*) T cells were transduced with A12 CAR targeted to PD-L1. (*C* and *D*) A12 CAR T cells recognized and killed B16 tumors. Coculture of anti–PD-L1 A12 CAR and a nonspecific control 1B7, recognizing a *T. gondii* calcium-dependent protein kinase, with B16 cells. Cells were cultured for 48 h at various effector:target (E:T) ratios. (*C*) A Cell Titer Glo assay was performed to measure cytotoxicity. (*D*) Supernatants were collected and IFNγ levels were measured. (*E* and *F*) A12 PD-L1–targeted cells were also effective in killing C3.43 HPV-transformed cancer cell lines. C3.43 cells were cultured with A12 CAR T cells at various E:T ratios. (*E*) C3.43 killing was measured by Cell Titer Glo, and (*F*) CAR activation was measured by IFNγ secretion. (*G* and *H*) A12 CAR T cells were cytotoxic against MC38 colon adenocarcinoma cells. A12 CAR T cells were cocultured with MC38 cells at various E:T ratios, and (*G*) MC38 killing and (*H*) A12 CAR T cell activation and cytokine secretion were measured. (*I* and *J*) Blocking experiments were performed using the B16 coculture setup. Cytotoxicity assay mixtures were incubated with varying concentrations soluble A12 VHH, B3 VHH, or an irrelevant 96G3M VHH (14). B3 binds PD-L1 with higher affinity than does A12. Higher levels of target antigen blockade lead to (*I*) better B16 survival and (*J*) less IFNγ secretion, indicating specificity. ****$P \leq 0.0001$.

adenocarcinoma, suggesting applicability across a spectrum of cancers. Cytotoxicity and IFNγ secretion again occurred in a dose-dependent manner. Both cytotoxicity (Fig. 2*I*) and IFNγ production (Fig. 2*J*) were blocked by inclusion of the corresponding soluble blocking VHH (B3), thus occluding other possible docking sites on the B16 melanoma for the CAR T cells to engage. We therefore conclude that cytotoxicity of the CAR T cells was specific for the target ligand.

Anti–PD-L1 CAR T Cells Are Generated More Effectively in a PD-L1–Deficient Background.

The design of CARs that recognize antigens expressed differentially on tumors versus normal cells poses a complication if the antigen is also expressed endogenously on the very same T cells programmed to display those CARs. This is the case for PD-L1, a possibly attractive target of solid tumors but expressed also at low levels on antigen-experienced T cells. We observed constitutively elevated IFNγ production when PD-L1–specific CARs were introduced into wild-type (WT), PD-L1–proficient T cells (Fig. 3*A*). Follicular T helper cells engage the PD-1/PD-L1 axis for proper function in the germinal center reaction (23). Consequently, "self"-activation of PD-L1–specific CAR T cells before they experience their targets could be problematic. Indeed, in the course of development of A12 CAR T cells, these cells showed enhanced expression of exhaustion markers such as PD1, TIM3, and LAG-3 (Fig. 3*B*), presumably due to chronic activation by PD-L1 engagement either in *cis* or in *trans*. Through introduction of PD-L1 CARs into PD-L1–deficient, activated T cells, such premature activation was avoided. PD-L1⁻/⁻ anti–PD-L1 CAR T cells also persisted better in vivo. PD-L1⁻/⁻ A12 PD-L1 CAR T cells or WT A12 PD-L1 CAR T cells were introduced into
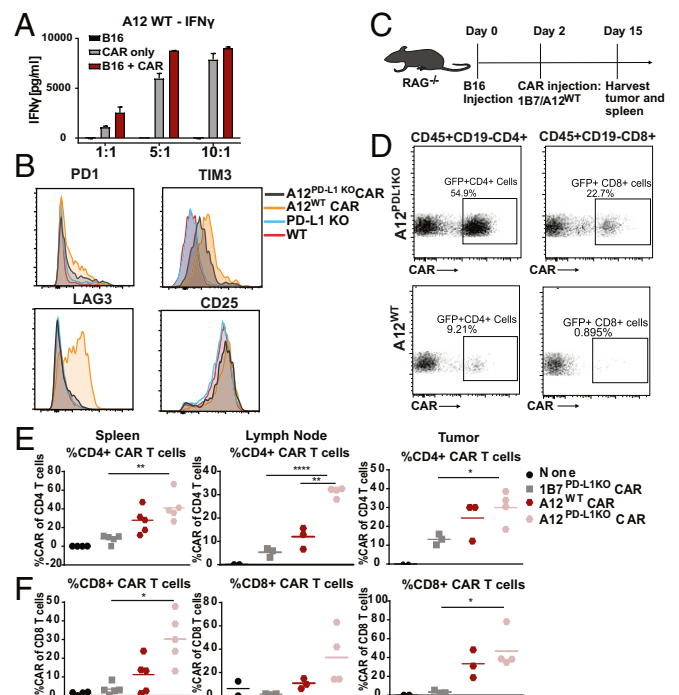

Fig. 3. Anti–PD-L1 CAR T cells are generated more effectively in a PD-L1–deficient background. (*A*) WT T cells were transduced with the A12 CAR and cultured with B16 cells for 48 h. Supernatants from the B16 coculture experiments were probed for levels of IFNγ. (*B*) A12 PD-L1–targeted CAR T cells were generated in WT T cells and PD-L1 KO T cells. A12 CAR T cells generated in WT T cells showed increased levels of PD1, TIM3, and LAG3 expression. (*C*) RAG⁻/⁻ mice were injected with B16 tumors s.c., and, 2 d later, A12 CAR T cells generated in WT T cells and PD-L1KO T cells were adoptively transferred. On day 15, tumors, spleens, and lymph nodes were harvested to determine the relative numbers of persisting CAR T cells. (*D*) Splenocytes were analyzed for the presence of GFP-labeled A12 CAR T cells. More CD4 and CD8 CAR T cells made in the PD-L1 KO background persisted. (*E*) Greater levels of CD4 CAR T cells made in the PD-L1 KO background were found in the spleen and draining lymph node (for 1B7 PD-L1⁻/⁻ vs. A12 PD-L1⁻/⁻: spleen CD4, $P = 0.0014$; spleen CD8, $P = 0.0023$; LN CD4, $P < 0.0001$; LN CD8, $P = 0.0757$; tumor CD4, $P = 0.0238$; tumor CD8, $P = 0.0162$; for A12 PD-L1⁻/⁻ vs. A12 WT: LN CD4, $P = 0.0007$). (*F*) More CD8 CAR T cells made in the PD-L1 KO background were present in the spleen, draining lymph nodes, and tumor. *$P \leq 0.05$, **$P \leq 0.01$, ***$P \leq 0.001$, ****$P \leq 0.0001$.

RAG$^{-/-}$ mice bearing B16 tumors, using 1B7 CAR T cells as controls (Fig. 3C). After 14 d of culture, spleens, tumors, and tumor-draining lymph nodes were harvested and probed for the presence of GFP+ CAR T cells. We saw that the A12 CAR CD4 and, to a lesser degree, CD8 T cells generated in a PD-L1$^{-/-}$ background expanded more in spleen and lymph nodes than A12 CAR T cells obtained from WT mice (Fig. 3 D–F). We also saw increased infiltration of PD-L1$^{-/-}$ CD8+ CAR T cells in the tumor compared with WT A12 CAR T cells or 1B7 (nonspecific) CAR T cells (Fig. 3 E and F). We conclude that persistent antigen recognition in the course of CAR T cell generation compromises activity and persistence of WT A12 CAR T cells in vivo. Interestingly, upon injection of varying amounts of A12 PD-L1$^{-/-}$ CAR T cells into WT hosts, we did not notice significant changes in the level of endogenous WT T cells, but did notice a decrease in CD45+CD11b+ cells in the spleen (*SI Appendix*, Fig. S2). This suggests that the level of PD-L1 expression, as well as the number of CAR T cells introduced, may determine whether cell killing occurs, or whether these T cells become exhausted.

In Vivo Application of Anti–PD-L1 CAR T Cells Slows Growth of Solid Tumors. Since PD-L1 is up-regulated on several cancer types, we determined whether A12 CAR treatment would affect growth of various tumor models known to overexpress PD-L1. The first model we tested was the highly aggressive B16 melanoma (Fig. 4A). C57BL/6 PD-L1$^{-/-}$ mice were inoculated with both WT B16 cells and B16 cells transfected to overexpress PD-L1 under the control of a CMV promoter (*SI Appendix*, Fig. S3). PD-L1$^{-/-}$ anti PD-L1 CAR T cells were injected into tumor-bearing mice once a week, for a total of three injections (9×10^6 to 14×10^6 cells per injection), using 1B7 CAR T cells as negative controls. Transduction rates of both CAR T cells were around 40% (*SI Appendix*, Fig. S1). TA-99, an anti-TRP1 monoclonal antibody that recognizes an antigen highly expressed on (a subset of) melanomas (30), was used in combination with CAR T cell treatment to enhance immune infiltration and delay tumor growth to allow the CAR T cells sufficient time to exert an effect. This aggressive melanoma model more accurately recapitulates human disease compared with standard NOD scid gamma (NSG) models, as the tumors are syngeneic and develop in the presence of a fully intact immune system, but with an ineffective immune response directed against the tumor. Mice treated with the A12 CAR T cells showed a statistically significant decrease in tumor growth rate and an increase in survival in both the B16 WT tumor model ($P < 0.0001$) and the PD-L1 overexpressing B16 model ($P = 0.02$) (Fig. 4 B–G). These experiments not only provide a system for studying CAR T cells in a syngeneic immunocompetent host but also avoid immune-depleting chemotherapy. We next tested A12 CAR T cell efficacy in the syngeneic MC38 model, in fully immunocompetent C57BL/6 mice (Fig. 4 H–J). Mice were inoculated with tumors and were left untreated or treated with either the A12 CAR T cells or the nonspecific 1B7 CAR T cells once a week, starting on day 5, for a total of three injections of 1×10^7 to 1.6×10^7 cells per injection. A12 CAR T cell treatment increased survival ($P = 0.003$), as well as decreasing tumor growth compared with either no treatment or untargeted treatment. Low levels of immunogenicity against the A12 CAR were seen in a few mice, but no visible side effects developed upon repeated administration. Immunogenicity did not adversely affect survival (*SI Appendix*, Fig. S4). Compared with mice actively immunized with VHHs, the levels of immunogenicity upon repeated CAR T cell injections are much lower (27, 28). A PD-L1–targeted VHH CAR T cell thus provides a significant survival benefit in several different tumor models. Immune checkpoints such as PD-L1 may serve as viable targets for CAR T cell therapy.
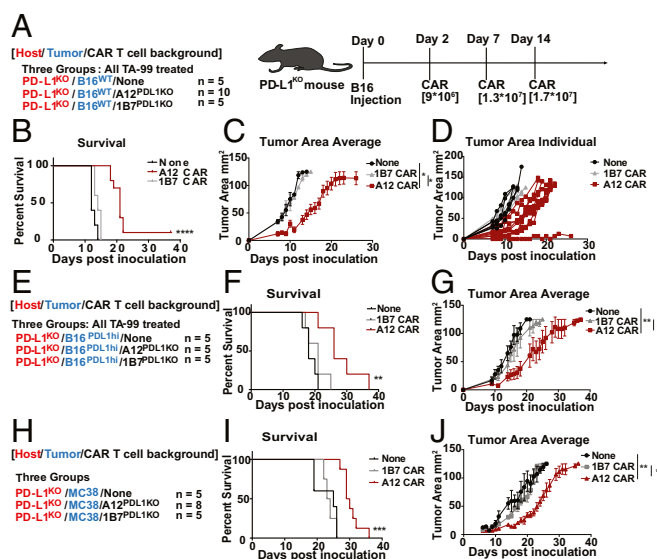

Fig. 4. In vivo application of anti–PD-L1 CAR T cells slows growth of solid tumors. (A) PD-L1 KO mice were inoculated with B16 tumor cells. On days 2, 7, and 14, mice were treated with A12 CAR T cells (n = 10) or 1B7-irrelevant CAR T cells (n = 5) or left untreated (n = 5). All mice were given an anti-TRP1 antibody, TA99, in combination with CAR T cell treatment. (B) Kaplan–Meier curves showing survival of each treatment condition (P < 0.0001, Mantel–Cox log-rank test). (C) The average tumor area with SEM and (D) individual tumor area of each mouse was measured. Treatment with the A12 CAR T cells delayed tumor growth (none/A12 P = 0.0296, 1B7/A12 P = 0.04). (E) PD-L1 KO mice were inoculated with B16 tumor cells engineered to express high levels of PD-L1 under the control of a CMV promoter (n = 5). (F) Kaplan–Meier curve showing survival of each group (P = 0.0233, Mantel–Cox log rank). Mice treated with A12 CAR T cells showed improved survival. (G) Average tumor area (none/A12 P = 0.0029, 1B7/A12 P = 0.0422, unpaired t test with Bonferroni correction) and individual tumor area for each group were measured. SEM is shown. (H) PD-L1 KO mice were inoculated with MC38 colon adenocarcinoma. Mice were either left untreated (n = 5), treated with irrelevant CAR T cells (n = 5), or treated with PD-L1–targeted CAR T cells (n = 8). (I) Survival was measured and plotted on a Kaplan–Meier curve, showing that A12 CAR treatment improved survival (P = 0.003). (J) The tumor area average for each group was monitored (none/A12 P = 0.003, 1B7/A12 P = 0.009, unpaired t test with Bonferroni correction).

Exhaustion of CAR T Cells Due to Persistent Activation Is Overcome by PD-L1 Blockade in Culture. Chronic PD-L1 exposure in the course of generating A12 CAR T cells decreases their persistence and proliferation. We reasoned that this phenomenon could be prevented by blocking PD-L1 exposure during culture. To prevent chronic activation of the A12 CAR T cells in culture, WT anti–PD-L1 CAR T cells were generated in the continuous presence of VHH B3, a high-affinity anti–PD-L1 VHH that blocks A12 binding of PD-L1 (27, 28). Indeed, blocking PD-L1 exposure in the course of CAR T cell generation decreases expression of exhaustion markers such as LAG3, TIM3, and PD-1 (Fig. 5A). We generated CAR T cells in either the WT or the PD-L1$^{-/-}$ background cultured with VHH B3 PD-L1 to prevent activation. We then introduced these A12 CAR T cells into WT C57BL/6 mice bearing a B16 tumor. After 2 wk, we harvested the spleens to determine persistence of CAR T cells. CD4 and, to a lesser extent, CD8 A12 CAR T cells generated in the presence of a PD-L1–blocking VHH expand more effectively in vivo than those generated in its absence (Fig. 5B). However, PD-L1$^{-/-}$ CAR T cells still proliferate more effectively. We next asked if decreasing the exhaustion level of these CAR T cells in the course of their production would improve an antitumor response in vivo. Mice inoculated with B16 tumors were treated with PD-L1–targeted CAR T cells generated in the WT background, but
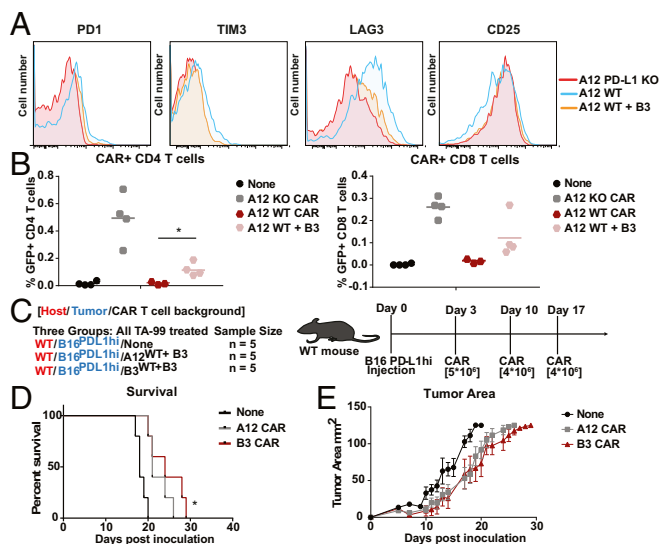
Fig. 5. Exhaustion of CAR T cells due to persistent activation overcome by PD-L1 blockade in culture. (*A*) Chronic antigen exposure and exhaustion of A12 CAR T cells made in a WT background can be blocked by incubation in the course of culture with soluble anti−PD-L1 VHH to mask endogenous PD-L1. A12 CAR T cells were generated in the presence of soluble B3 VHH, which binds PD-L1 with higher affinity than A12. Expression of common exhaustion markers was analyzed using flow cytometry. (*B*) WT mice were inoculated with B16 tumors, and A12 CAR T cells made in a WT background with and without inclusion of soluble B3 were introduced and compared with A12 CAR T cells made in the PD-L1 KO background. A12 CAR T cells made in a WT background in the presence of soluble B3 showed better persistence than A12 CAR T cells made without inclusion of B3 (CD4: A12 WT vs. A12 WT+ B3, *P* = 0.0283; CD8: A12 WT vs. A12 WT+ B3, *P* = 0.1346). (*C*) Mice were inoculated with B16 overexpressing PD-L1 tumors on day 0, and either A12 or B3 CAR T cells generated in the presence of soluble B3 were introduced on days 3, 10, and 17 (*n* = 5). (*D*) Kaplan−Meier curve showing survival of each group. Mice treated with the A12 and B3 CAR T cells showed a slight increase in survival (*P* = 0.0058, Mantel−Cox log-rank test). (*E*) Individual tumor area for each group was measured. The A12 CAR T cells generated in the presence of soluble B3 slightly delayed tumor growth (*P* = 0.0483). SEM is shown. **P* ≤ 0.05, ***P* ≤ 0.01.

cultured in the presence of excess soluble anti−PD-L1 VHH to prevent chronic activation (Fig. 5*C*). Since the in vitro data showed inferiority, we did not test the PD-L1−targeted CARs generated in the WT background without PD-L1 blocking. We observed a delay in B16 tumor growth in mice that received WT anti−PD-L1 CAR T cells generated in the presence of the PD-L1−blocking VHH (*P* = 0.04) (Fig. 5 *D* and *E*), showing that the prevention of early activation in culture is a viable means of allowing a PD-L1−targeted CAR T cell to be deployed in a patient setting.

Anti-EIIIB Fibronectin-Targeted CAR T Cells Slow B16 Melanoma Growth in Vivo. EIIIB is an alternatively spliced domain of fibronectin strongly expressed in tumors and during angiogenesis, but not in most normal tissues (26). We targeted CAR T cells specifically to the tumor microenvironment (stromal ECM and neovasculature) through recognition of the fibronectin EIIIB+ splice variant. We used VHH NJB2, which targets EIIIB (29), to generate B2 CAR T cells, and transduction rates of the B2 CAR were around 80% (*SI Appendix*, Fig. S1). We determined display of the B2 CAR by flow cytometry, using recombinant EIIIB-GST as the ligand and probing with rabbit anti-GST and fluorescently labeled anti-rabbit (Fig. 6*A*). Coculture of B2 CAR T cells with aortic endothelial cell lines that either contain or lack the EIIIB domain (gift from R.O.H.) confirm their specificity and cytotoxicity in vitro (Fig. 6*B*). Immunohistochemistry (IHC) and PET

imaging of B16 tumors show that EIIIB is present in their tumor stroma and neovasculature (29). We therefore used the B16 melanoma model to show that treatment with B2 CAR T cells delays tumor growth. Mice were injected s.c. with 1×10^5 B16 melanoma cells without prior lymphodepletion. Four days after tumor inoculation, a total of three CAR T cell injections [1×10^7 to 1.5×10^7 cells] were given at weekly intervals (Fig. 6*C*). The B2 CAR T cells successfully delayed tumor growth and improved survival (*P* = 0.0001) compared with treatment with nonspecific CAR T cells (Fig. 6*D*). The B2 CAR T cell treatment was then combined with the anti-TRP1 antibody, TA99, to try to further enhance innate immune infiltration (*SI Appendix*, Fig. S6). Low levels of immunogenicity against the B2 CAR were seen in a few mice, but no visible side effects developed upon repeated administration, and immunogenicity was not related to survival (*SI Appendix*, Fig. S4). B2 CAR T cell treatment was also tested in a B16 model in immunocompromised RAG$^{-/-}$ mice to determine the contribution of the endogenous adaptive immune system in the efficacy of treatment (Fig. 6*E*). We saw no significant increase
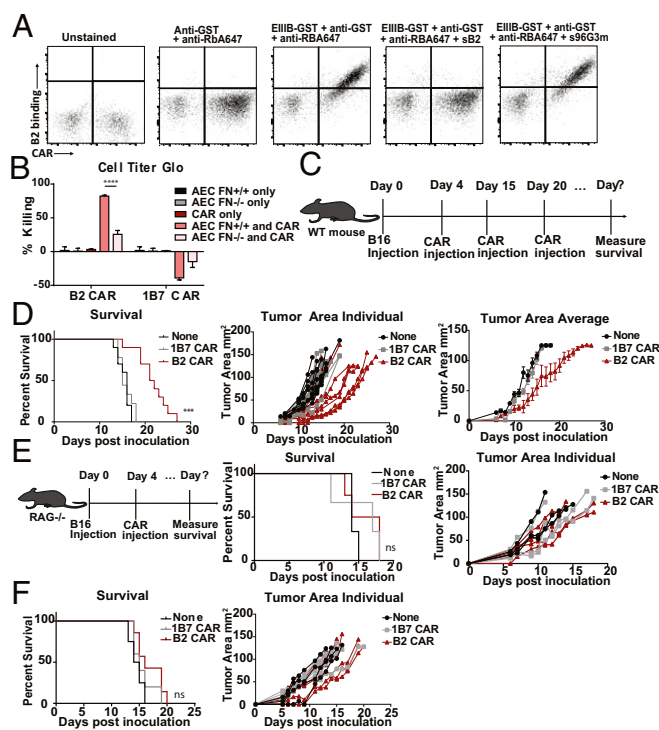

Fig. 6. Anti-EIIIB fibronectin-targeted CAR T cells slow B16 melanoma growth in vivo. (*A*) T cells were transduced with the EIIIB-specific B2 CAR construct, and transduction efficiency was monitored by mCherry expression. Cells were then incubated with recombinant EIIIB-GST and probed with rabbit anti-GST and anti-rabbit A647 to determine ligand binding. (*B*) B2 CAR T cells show cytotoxicity in response to ligand recognition. B2 CAR T cells were cocultured with aortic endothelial cells (AEC) that either express the EIIIB fibronectin domain (AEC FN$^{+/+}$) or lack it (AEC FN$^{-/-}$). (*C*) Mice were inoculated with B16 tumors on day 0, and B2 CAR T cells (*n* = 10) were introduced on days 4, 15, and 20. (*D*) Tumor area was measured for individual mice. Kaplan−Meier curve showing survival of each group (*P* = 0.0001, Mantel−Cox log-rank test with the Bonferroni correction for multiple comparisons). Mice treated with the B2 CAR T cells showed improved survival. SEM is shown. (*E*) RAG$^{-/-}$ mice were inoculated with B16 tumors and treated with B2 (*n* = 4) or 1B7 CAR T cells (*n* = 3) on day 4. RAG$^{-/-}$ mice treated with B2 CAR T cells do not show improved survival increase or delayed tumor growth. SEM is shown. (*F*) MC38 expresses lower levels of EIIIB (*SI Appendix*, Fig. S8). MC38 survival curves (*P* = 0.1895, ns, Mantel−Cox log-rank test) and MC38 individual tumor areas were not significantly affected by treatment with B2 CAR T cells (*n* = 7). ****P* ≤ 0.001, *****P* ≤ 0.0001; ns, nonsignificant.

in survival or delay in tumor growth when tumor-bearing mice lacking adaptive immunity were treated with the B2 CAR T cells, despite efficient expansion of the B2 CAR T cells (*SI Appendix*, Fig. S7), indicating that the CAR treatment synergizes with the endogenous adaptive immune system to show efficacy in these immunocompetent tumor models. To further test the degree of efficacy of B2 CAR T cells in tumors with lower expression levels of EIIIB, we also investigated the MC38 colon carcinoma model. From immunohistological examination of excised MC38 tumors, we observed only low levels of EIIIB expression compared with the levels on B16 tumors (*SI Appendix*, Fig. S8). Mice inoculated with MC38 tumors and treated with B2 CAR T cells showed minimal effects on survival or tumor growth (Fig. 6F). We therefore suggest that the poor efficacy of B2 CAR T cells in the MC38 model is likely due to this lower expression level of EIIIB and that, for the B2 CAR T cells to be effective, a minimum level of EIIIB expression is required. These results show that targeting CAR T cells selectively to tumor ECM and neovasculature can be very effective in suppressing tumor growth. We conclude that we can apply VHHs to generate CAR T cells that are effective in vivo against targets in the tumor microenvironment in fully immunocompetent mice.

Treatment with Anti-EIIIB Fibronectin-Targeted CAR T Cells Leads to Tumor Immune Infiltration and Necrosis.

To more closely analyze the mechanisms of B2 CAR treatment, we performed IHC on tumors excised while undergoing treatment. WT C57BL/6 mice were inoculated with B16 tumors, and mice were either treated with B2 CAR T cells or left untreated. At day 16, when there was a significant difference in tumor sizes between the treated and control group (Fig. 7 A and B), tumors were excised, fixed, and subjected to IHC. Tumor samples were then stained with secondary only (control) or for EIIIB, CD31, CD3, CD4, and CD8 to determine how ECM, vasculature, and immune cell populations were affected by the B2 CAR T cell treatment. The structure of the untreated tumors appeared healthy and intact, while the treated tumors showed clear signs of disruption. In the untreated samples, we saw expression of EIIIB in the tumor stroma and capsule, as well as around the vasculature, as indicated by its partial colocalization with CD31 (Fig. 7C). Expression of EIIIB in the tumor stroma appeared heterogeneous. In contrast, two of the three smaller treated tumors were highly necrotic, as indicated by the lack of healthy nuclear staining and disintegration of the matrix (Fig. 7D). Furthermore, these two treated samples showed decreased levels of CD31-positive vasculature compared with controls. Since B2 CAR T cells are targeted to EIIIB, which is expressed in tumor stroma and on neovasculature, the necrotic nature and lack of CD31 expression in the treated samples is perhaps to be expected. The third treated tumor was slightly larger (Fig. 7B) and was heterogeneous, showing a mixture of live, healthy tumor and necrotic, damaged tissue (Fig. 7E, *Top*). The healthy tumor regions expressed EIIIB and showed heavy T cell infiltration throughout the tissue, compared with untreated tumors. CD31 staining of this heterogeneous tumor indicated the presence of intact vasculature in the healthy sections with immune cell infiltration, while the necrotic regions displayed a lack of vasculature with less T cell infiltration (Fig. 7E, *Bottom*). Averaging across all tumors, those treated with B2 CAR T cells had elevated levels of immune cells (Fig. 7F). The heterogeneous treated tumor showed many more infiltrating immune cells in those regions that were still alive (Fig. 7G). A reasonable interpretation is that the B2 CAR T cells infiltrate the tumors and possibly also recruit additional immune cells. These data further corroborate the ability of B2 CAR T cells to infiltrate and damage EIIIB-expressing tumors. Tumors rely on support and nutrients delivered by their stroma and vasculature, and, by compromising these interactions, the B2 CAR T cells markedly delay tumor growth.
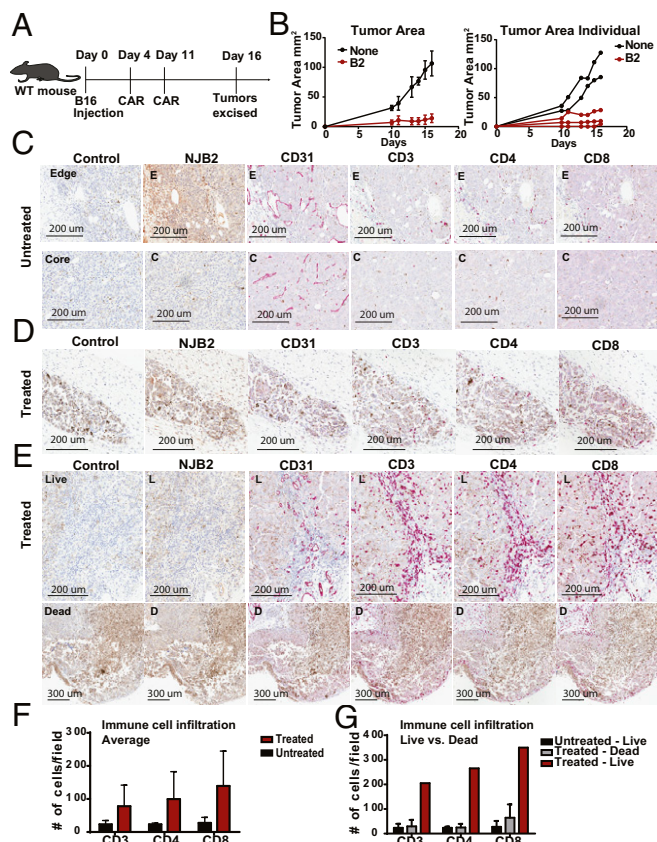

Fig. 7. Treatment with anti-EIIIB fibronectin-targeted CAR T cells leads to tumor immune infiltration and necrosis. (A) WT mice were inoculated with tumors on day 0 and either left untreated (N = 2) or treated with B2 CAR T cells (n = 3) twice, on days 4 and 11. On day 16, tumors were harvested, fixed, and embedded for IHC and stained for EIIIB, CD31, CD3, CD4, and CD8. (B) The tumor area average measurements and values for individual mice are plotted. (C) Tumor samples were stained with PBS and secondary only (control), NJB2 VHH, anti-CD31, anti-CD3, anti-CD4, and anti-CD8. One representative image is shown. A 20× magnification of the edge (E), capsular region (*Top*) of the tumor is shown. A similar magnification of a core (C) (*Bottom*) regions of the tumor is shown. EIIIB is present in the tumor capsule, tumor stroma, and surrounding the tumor vasculature, as inferred from colocalization with CD31 staining. In untreated samples, tumors appeared healthy and live, with intact matrix throughout the tissue. Little T cell and immune infiltration was apparent. (D) Necrotic B2 CAR T cell-treated tumors. Two of the three smaller treated tumors were highly necrotic, with a disintegrated matrix. CD31 staining shows a lack of tumor vasculature with little immune infiltration. (E) One treated tumor appeared to be heterogeneous and showed both (*Bottom*) necrotic [dead (D)] and (*Top*) live (L) sectors. The live tissue showed CD31 staining and was heavily infiltrated by CD3-, CD4-, and CD8-positive cells. (F) The number of CD3-, CD4-, and CD8-positive cells was quantified for both treated and untreated tumors. (G) The number of CD3-, CD4-, and CD8-positive cells was quantified for both the live and dead sections of the treated and untreated tumors.

Discussion

Although CAR T cells have shown success in treating several types of hematological cancers, their deployment will require further refinement for an attack on solid tumors. Limitations in biomarker availability, insufficient delivery of CAR T cells, and an increased immunosuppressive environment within the tumor may account for poor CAR T cell performance in the treatment of solid tumors (31). Physical barriers, such as a dense ECM that encapsulates the tumor, or properties of the vasculature that preclude adhesion and diapedesis of CAR T cells could likewise compromise their efficacy (31). Indeed, many solid tumors

suppress immunity through expression of checkpoint proteins such as PD-L1, which engage corresponding inhibitory receptors on T cells (23). PD-L1 has not been exploited as a target for CAR T cells in vivo.

Establishing a more inflammatory local environment might be beneficial to overcoming immune suppression. Monoclonal antibodies that inhibit development of the tumor vasculature by targeting VEGF, or cytokine therapies such as provision of IL2 or IL-12, can increase inflammation in the tumor for more effective immune control (27, 32–34). Cytokine release by activated CAR T cells might help establish the requisite local conditions, in addition to exerting their cytolytic effects. We therefore generated CAR T cells that either target the checkpoint protein PD-L1 or the tumor stromal ECM and neovasculature through EIIIB, a fibronectin splice variant strongly expressed in both murine and human tumors, both recognized by NJB2 VHH (25, 29). A major difficulty in developing CAR T cells for solid tumor treatment is the lack of targetable antigens. Most antigens proposed as CAR T cell targets to treat solid tumors are exclusive to a specific cancer type, and limited information on cancer-specific antigens for the vast majority of solid tumors puts many tumors out of reach for CAR T cell therapy (35). By targeting markers in the tumor microenvironment that are expressed in a variety of tumors, the CAR T cells described here show versatility for several different tumor models. They have the potential to target other cancers that lack identified tumor-specific antigens. PD-L1 is overexpressed on a majority of tumors and on immune cells within the tumor microenvironment (36). EIIIB is expressed in the neovasculature and tumor stroma of a range of tumor subtypes (25). The EIIIB-targeted VHH has already been tested against a panel of multiorgan human tissue metastasis biopsies and reacts with a diverse set of tumor samples, further demonstrating the possible broad applicability of the B2 CAR T cells (29).

We optimized the production of VHH-based CAR T cells and verified their function in vitro and in vivo by direct ligand-binding assays, cytotoxicity, cytokine production, and inhibition of tumor growth. VHH-based CAR T cells that recognize PD-L1 show ligand-specific cytotoxicity and are effective in highly aggressive, syngeneic tumor models in immunocompetent mice without prior immunodepletion. As long as the immune system contributes to eradication of solid tumors, as in the case of melanoma, lymphodepletion may have significant deleterious effects. We suggest that the mode of action for these PD-L1 targeted CAR T cells is at least twofold. First, anti–PD-L1 CAR T cells exert direct cytotoxicity and produce cytokines. Second, binding of a CAR to the relevant checkpoint molecules should block their interaction with natural ligands on host T cells, resulting in less immune suppression and exhaustion. In vitro, PD-L1−targeted CAR T cells show cytotoxicity against several types of solid tumors, including B16 melanoma, MC38 colon adenocarcinoma, and C3.43 HPV-transformed cell lines. In vivo, PD-L1−targeted CAR T cells significantly inhibit growth of B16 and MC38 tumors and provide a survival benefit.

The production of anti–PD-L1 CAR T cells is complicated by the fact that WT T cells express low, endogenous levels of PD-L1. Anti–PD-L1 CAR T cells generated in the WT background therefore constantly experience low levels of antigen exposure. This leads to some degree of T cell exhaustion and impairs function, in vivo persistence, and proliferation of the CAR T cells. This phenomenon is not unique to the PD-L1 target, as several desirable tumor antigens are also expressed at low levels elsewhere in the tumor, because, with the exception of neoantigens, very few truly tumor-specific antigens exist. We found two ways to overcome this hurdle. First, mice treated with anti–PD-L1 CAR T cells generated in a PD-L1−deficient background showed a delay in tumor growth, indicating that these VHH-based CAR T cells are indeed effective in tumor treatment. Second, by generating anti–PD-L1 CAR T cells in the continuous presence of a saturating dose of an anti−PD-L1

VHH in solution, engagement of the PD-1/PD-L1 axis is blocked, and the resulting CAR T cells retain efficacy in vivo. Genetic ablation of PD-L1 using CRISPR-Cas9 in the course of CAR generation would likewise be possible, but involves genetic modifications in addition to provision of the CAR construct (37). We therefore preferred provision of the CAR ectodomain in soluble form in the course of generating anti−PD-L1 CAR T cells. In our experiments, we saw no obvious untoward effects upon transfer of these CAR T cells at our injection levels. We noticed a decrease in CD11b+ cells, which were highly PD-L1−positive, but did not see significant changes in other immune populations. Generation of the PD-L1−targeted CAR T cells in a WT background did not result in fratricide, possibly due to sequestering of the PD-L1 ligand by PD1 on the T cell surface in *cis*, as reported for antigen presenting cells (APCs) (38), or an insufficient level of PD-L1 expression to induce killing.

Targeting the tumor ECM or neovasculature in the tumor microenvironment rather than the tumor directly may serve as another method to target multiple tumor types. Since most solid tumors require angiogenesis to provide nutrients for survival, targeting stromal and neoangiogenic markers may be a viable strategy (39). Indeed, an EIIIB$^+$ fibronectin CAR (B2 CAR) T cell targeted to tumor ECM and the neovasculature inhibited growth of the aggressive B16 melanoma in an immunocompetent mouse. B16 tumors are strongly positive for EIIIB as assessed by IHC. B2 CAR T cell-treated B16 tumors are largely necrotic and show vascular and stromal damage, delaying tumor growth, as fewer nutrients can be delivered to support tumor growth. Treated tumor tissue that is not already necrotic shows immune cell infiltration, suggesting that B2 CAR T cells and possibly other endogenous immune cells localize to damaged tumor ECM and vasculature. In contrast, the MC38 tumor, which showed less expression of the EIIIB fibronectin splice variant, failed to respond to treatment with anti-EIIIB CAR T cells. Even though solid tumors may share a need for ECM and angiogenesis, not all tumors display the FN EIIIB variant equally. It may be possible to identify other vascular and stromal markers that might serve a similar purpose. These B2 CAR T cell models further highlight the importance of using syngeneic animal models for CAR T cell treatment. When RAG$^{-/-}$ mice inoculated with B16 were treated with B2 CAR T cells, the survival benefit was lost, highlighting the importance of the endogenous immune system in synergizing with CAR treatment. Unlike the B2 CAR T cell treatment, when the A12 CAR T cell treatment was tested in RAG$^{-/-}$ mice, we noticed a survival benefit. As PD-L1 is expressed by the actual tumor cells, unlike EIIIB, a survival benefit would be expected. However, with the EIIIB-targeted CAR T cell treatment, it may be possible that compromising the matrix allows for greater immune infiltration and buildup of an endogenous immune response to antigens directly on the tumor itself, explaining why treatment was effective in immunocompetent mice but not in immunodeficient mice.

Targeting the tumor neovasculature and tumor stroma with EIIIB-targeted CAR T cells may not only compromise the blood supply of the tumor, it might also serve as a means for improving tumor accessibility for small-molecule drugs and other therapies that can be used in combination with the CAR T cells, even if only transiently. Much like therapies that combine different checkpoint-blocking antibodies, the most likely route forward for solid tumors lies in combinations of CAR T cells with antibodies, radiation, or small-molecule drugs. From our experiments with both the PD-L1−targeted and EIIIB-targeted CAR T cells, we conclude that the VHH-based CAR approach is highly modular and broadly applicable to various tumors. Once a VHH of the appropriate specificity has been identified, it can be slotted into the CAR backbone for expression without the need for modification and optimization of linkers that connect V_H and V_L, which are an integral part of scFv-based CAR T cells. A platform for producing VHH-based CAR T cells expands the range of syngeneic tumors targetable by CAR T cells in a fully immunocompetent murine model. VHHs are appealing as antigen

recognition domains for CAR T cells, as they are easily expressible and have no obvious stability concerns (9, 11, 40–42).

Immunodeficient mouse models are still largely the most commonly used models in CAR T cell research (43–45). They are beneficial in that human tumor models and CAR T cells can be studied, but also suffer from a number of drawbacks. Without the presence of intact innate and adaptive immunity, these animal models do not accurately depict the potential of immune suppression that may occur in the clinic. The use of immunocompetent mice as a tumor model has the added benefit of endogenous immunity and more accurately depicts clinical effects and recapitulates the degree of efficacy. Development of therapies that do not require immune depletion would seem further desirable, as endogenous antitumor immunity plays a large role in tumor surveillance (46). Compared with xenograft models, immunocompetent models also allow for better assessment of the safety profile of treatment.

The results from these models demonstrate feasibility and efficacy of CAR T cells that target the tumor microenvironment against aggressive solid tumors in a fully immunocompetent system. Our models show generalizability across multiple tumor types. Future efforts should be directed at incorporation of combination therapies, including checkpoint blockade and cytokine therapies to further improve treatment of solid tumors.

Materials and Methods

CAR T cells were generated through retroviral infection of primary murine T cells. In vitro assays were performed using Cell Titer Glo (Promega) and IFNγ and IL-2 ELISAs (BD). All animal procedures performed were in accordance with institutional guidelines and approved by the Institutional Animal Care and Use Committee of Boston Children's Hospital (IACUC Protocol 16-12-3328). A detailed description of the materials and methods used in this study is provided in SI Appendix, Supplementary Materials and Methods.

1. Porter DL, Levine BL, Kalos M, Bagg A, June CH (2011) Chimeric antigen receptor-modified T cells in chronic lymphoid leukemia. N Engl J Med 365:725–733.
2. Maude SL, et al. (2014) Chimeric antigen receptor T cells for sustained remissions in leukemia. N Engl J Med 371:1507–1517.
3. Maher J, Brentjens RJ, Gunset G, Rivière I, Sadelain M (2002) Human T-lymphocyte cytotoxicity and proliferation directed by a single chimeric TCRzeta/CD28 receptor. Nat Biotechnol 20:70–75.
4. Sadelain M, Brentjens R, Rivière I (2013) The basic principles of chimeric antigen receptor design. Cancer Discov 3:388–398.
5. Savoldo B, et al. (2011) CD28 costimulation improves expansion and persistence of chimeric antigen receptor-modified T cells in lymphoma patients. J Clin Invest 121:1822–1826.
6. Eshhar Z, Waks T, Gross G, Schindler DG (1993) Specific activation and targeting of cytotoxic lymphocytes through chimeric single chains consisting of antibody-binding domains and the gamma or zeta subunits of the immunoglobulin and T-cell receptors. Proc Natl Acad Sci USA 90:720–724.
7. Wörn A, Plückthun A (1999) Different equilibrium stability behavior of ScFv fragments: Identification, classification, and improvement by protein engineering. Biochemistry 38:8739–8750.
8. Sun W, et al. (2012) A combined strategy improves the solubility of aggregation-prone single-chain variable fragment antibodies. Protein Expr Purif 83:21–29.
9. Revets H, De Baetselier P, Muyldermans S (2005) Nanobodies as novel agents for cancer therapy. Expert Opin Biol Ther 5:111–124.
10. Ingram JR, Schmidt FI, Ploegh HL (2018) Exploiting nanobodies' singular traits. Annu Rev Immunol 36:695–715.
11. De Meyer T, Muyldermans S, Depicker A (2014) Nanobody-based products as research and diagnostic tools. Trends Biotechnol 32:263–270.
12. Vincke C, et al. (2009) General strategy to humanize a camelid single-domain antibody and identification of a universal humanized nanobody scaffold. J Biol Chem 284:3273–3284.
13. Ditlev SB, et al. (2014) Utilizing nanobody technology to target non-immunodominant domains of VAR2CSA. PLoS One 9:e84981.
14. Ingram JR, et al. (2017) PD-L1 is an activation-independent marker of brown adipocytes. Nat Commun 8:647.
15. Kirchhofer A, et al. (2010) Modulation of protein properties in living cells using nanobodies. Nat Struct Mol Biol 17:133–138.
16. Ingram JR, et al. (2015) Allosteric activation of apicomplexan calcium-dependent protein kinases. Proc Natl Acad Sci USA 112:E4975–E4984.
17. Porter DL, et al. (2015) Chimeric antigen receptor T cells persist and induce sustained remissions in relapsed refractory chronic lymphocytic leukemia. Sci Transl Med 7:303ra139.
18. Kowolik CM, et al. (2006) CD28 costimulation provided through a CD19-specific chimeric antigen receptor enhances in vivo persistence and antitumor efficacy of adoptively transferred T cells. Cancer Res 66:10995–11004.
19. Morgan RA, et al. (2010) Case report of a serious adverse event following the administration of T cells transduced with a chimeric antigen receptor recognizing ERBB2. Mol Ther 18:843–851.
20. Gong MC, et al. (1999) Cancer patient T cells genetically targeted to prostate-specific membrane antigen specifically lyse prostate cancer cells and release cytokines in response to prostate-specific membrane antigen. Neoplasia 1:123–127.
21. Cheung NK, Guo HF, Modak S, Cheung IY (2003) Anti-idiotypic antibody facilitates scFv chimeric immune receptor gene transduction and clonal expansion of human lymphocytes for tumor therapy. Hybrid Hybridomics 22:209–218.
22. Iwai Y, et al. (2002) Involvement of PD-L1 on tumor cells in the escape from host immune system and tumor immunotherapy by PD-L1 blockade. Proc Natl Acad Sci USA 99:12293–12297.
23. Blank C, et al. (2004) PD-L1/B7H-1 inhibits the effector phase of tumor rejection by T cell receptor (TCR) transgenic CD8+ T cells. Cancer Res 64:1140–1145.
24. Astrof S, et al. (2004) Direct test of potential roles of EIIIA and EIIIB alternatively spliced segments of fibronectin in physiological and tumor angiogenesis. Mol Cell Biol 24:8662–8670.
25. Neri D, Bicknell R (2005) Tumour vascular targeting. Nat Rev Cancer 5:436–446.
26. Castellani P, et al. (1994) The fibronectin isoform containing the ED-B oncofetal domain: A marker of angiogenesis. Int J Cancer 59:612–618.
27. Dougan M, et al. (2018) Targeting cytokine therapy to the pancreatic tumor microenvironment using PD-L1-specific VHHs. Cancer Immunol Res 6:389–401.
28. Ingram JR, et al. (2017) Localized CD47 blockade enhances immunotherapy for murine melanoma. Proc Natl Acad Sci USA 114:10184–10189.
29. Jailkhani N, et al. (2018) Non-invasive imaging of tumor progression, metastases and fibrosis using a nanobody targeting the extracellular matrix. Proc Natl Acad Sci USA.
30. Martínez-Esparza M, Jiménez-Cervantes C, Solano F, Lozano JA, García-Borrón JC (1998) Mechanisms of melanogenesis inhibition by tumor necrosis factor-alpha in B16/F10 mouse melanoma cells. Eur J Biochem 255:139–146.
31. Shiao SL, Ganesan AP, Rugo HS, Coussens LM (2011) Immune microenvironments in solid tumors: New targets for therapy. Genes Dev 25:2559–2572.
32. Belo AV, Barcelos LS, Teixeira MM, Ferreira MAND, Andrade SP (2004) Differential effects of antiangiogenic compounds in neovascularization, leukocyte recruitment, VEGF production, and tumor growth in mice. Cancer Invest 22:723–729.
33. Ting CC, Yang SS (1982) Effect of interleukin 2 on cytotoxic effectors: I. Short-term culture of the cytotoxic effectors and the in vivo anti-tumor activity of the cultured effectors isolated from tumor site. Int J Cancer 30:625–632.
34. Brunda MJ, et al. (1993) Antitumor and antimetastatic activity of interleukin 12 against murine tumors. J Exp Med 178:1223–1230.
35. Dotti G, Gottschalk S, Savoldo B, Brenner MK (2014) Design and development of therapies using chimeric antigen receptor-expressing T cells. Immunol Rev 257:107–126.
36. Pardoll DM (2012) The blockade of immune checkpoints in cancer immunotherapy. Nat Rev Cancer 12:252–264.
37. Rupp LJ, et al. (2017) CRISPR/Cas9-mediated PD-1 disruption enhances anti-tumor efficacy of human chimeric antigen receptor T cells. Sci Rep 7:737.
38. Zhao Y, et al. (2018) Antigen-presenting cell-intrinsic PD-1 neutralizes PD-L1 in cis to attenuate PD-1 signaling in T cells. Cell Rep 24:379–390.e6.
39. Pietras K, Ostman A (2010) Hallmarks of cancer: Interactions with the tumor stroma. Exp Cell Res 316:1324–1331.
40. De Munter S, et al. (2018) Nanobody based dual specific CARs. Int J Mol Sci 19:E403.
41. Khaleghi S, Rahbarizadeh F, Ahmadvand D, Rasaee MJ, Pognonec P (2012) A caspase 8-based suicide switch induces apoptosis in nanobody-directed chimeric receptor expressing T cells. Int J Hematol 95:434–444.
42. Iri-Sofla FJ, Rahbarizadeh F, Ahmadvand D, Rasaee MJ (2011) Nanobody-based chimeric receptor gene integration in Jurkat cells mediated by φC31 integrase. Exp Cell Res 317:2630–2641.
43. Johnson LA, et al. (2015) Rational development and characterization of humanized anti-EGFR variant III chimeric antigen receptor T cells for glioblastoma. Sci Transl Med 7:275ra22.
44. Craddock JA, et al. (2010) Enhanced tumor trafficking of GD2 chimeric antigen receptor T cells by expression of the chemokine receptor CCR2b. J Immunother 33:780–788.
45. Wilkie S, et al. (2008) Retargeting of human T cells to tumor-associated MUC1: The evolution of a chimeric antigen receptor. J Immunol 180:4901–4909.
46. Fong L, et al. (2009) Potentiating endogenous antitumor immunity to prostate cancer through combination immunotherapy with CTLA4 blockade and GM-CSF. Cancer Res 69:609–615.